ISSN 1330–0008
CODEN FIZAE4

STRUCTURAL AND ELECTRICAL PROPERTIES OF $CuSbTe_2$, $CuSbSe_2$ AND $CuSbS_2$ CHALCOGENIDE THIS FILMS

LAILA I. SOLIMAN[a], AZIZA M. ABO EL SOAD[a], HAMDIA A. ZAYED[b] and SAMMER A. EL GHFAR[b]

[a]*National Research Centre, Solid State Physics Department, Dokki, Cairo, Egypt*

[b]*Girls College for Art, Science and Education, Ain Shams University*

Received 9 January 2002; revised manuscript received 2 July 2002
Accepted 11 November 2002 Online 7 February 2003

The ternary chalcogenides $CuSbTe_2$, $CuSbSe_2$ and $CuSbS_2$ were synthesized by the direct fusion technique. The thin films of these compounds were prepared by thermal evaporation under vacuum of about 1.3 mPa (10^{-5} Torr) and the rate of deposition was 30 nm/min. The structural properties of $CuSbTe_2$, $CuSbSe_2$ and $CuSbS_2$ in powder and thin film forms were investigated by X-ray diffraction (XRD) and transmission electronmicroscopy. Microprobe analysis technique was used to investigate the composition of the three alloys and of their films. The electrical conductivity σ and the thermoelectrical power Q have been measured for all as-deposited and annealed thin films, as a function of temperature in the range from 80 to 500 K. It was found that the electrical conductivity σ, the carrier concentration P, the mobility μ and the thermoelectric power Q increase when increasing the annealing temperature for $CuSbTe_2$, $CuSbSe_2$ and $CuSbS_2$ thin films. The increase of σ, P, μ and Q, and also the decrease of the activation energy ΔE with increasing temperature for the as-deposited $CuSbTe_2$, $CuSbSe_2$ and $CuSbS_2$ thin films, can be attributed to the change in the structure of these films from the amorphous to the crystalline state.

PACS numbers: 61.10.-i, 73.50.-h UDC 538.975

Keywords: ternary chalcogenides $CuSbTe_2$, $CuSbSe_2$ and $CuSbS_2$, thin films, amorphous, crystalline, as-deposited, annealed, electrical conductivity, Hall effect, thermoelectrical power, carrier concentration, mobility, activation energy

1. Introduction

Recently, a considerable effort has been invested to gain a better and deeper understanding of structural, electrical and optical properties of ternary chalcogenide semiconductors because of their possible applications in electrical devices and infrared generation and detection [1]. Ternary chalcogenide compounds $A^{I}B^{V}X_2^{IV}$ (A = Cu, B = Sb, X = Te, Se or S) can be regarded as valence analogues of III - V and II - VI semiconductors [2] and they crystallize in the chalcogenide structure [3,4] which is closely related to the zinc blende. The structure and chemical bonding of compounds of the type $A^{I}B^{V}X_2^{IV}$ have been discussed by Hofmann [5]. It has been shown that the atom B comes from the group V (Sb), while the atom A (Cu) is octahedrally surrounded by X (Te, Se or S) atoms. It is likely that the chemical bonds in the compounds of this system are formed by the d–$5p_2$ hybridised orbitals in which the d-electrons are contributed by the copper atoms.

$CuSbTe_2$, $CuSbSe_2$ and $CuSbS_2$ compounds have recently received renewed interest as infrared materials for infra-red detectors and in solar energy applications [6-9]. To evaluate these materials for such applications, their structural, optical, electrical and photoconductivity properties should be thoroughly understood. The preparation and the crystal structure of $CuSbTe_2$, $CuSbSe_2$ and $CuSbS_2$ compounds have been reported by many workers [6,9-11], but their transport properties in the solid state has been described very little [12-15]. To our knowledge, there are no published studies on the transport properties of $CuSbTe_2$, $CuSbSe_2$ and $CuSbS_2$ thin films.

In this paper, we describe the electrical and thermoelectric properties of $CuSbTe_2$, $CuSbSe_2$ and $CuSbS_2$ thin films as functions of temperature for different thicknesses and at different annealing temperatures, and study the structure of these compounds in both powder and thin-film forms.

2. *Experimental*

$CuSbTe_2$, $CuSbSe_2$ and $CuSbS_2$ compounds were synthesized by the fusion method. In this method, the reaction between the chalcogenide vapours and molten metals were allowed to take place gradually in evacuated silica tubes. High purity (99.999%) mixtures of constituent elements (Cu, Sb, and Te, Se or S) in stoichiometric proportions (with an accuracy of 5×10^{-4} g) were sealed into evacuated and graphitized silica tubes at the pressure of 1.3 mPa (10^{-5} Torr). The evacuated tube was then placed into a furnace whose temperature was raised in steps to 1150 K for 50 hours. During the synthesis, the molten material was vibration shaken to ensure homogeneity. The tubes were gradually cooled with a cooling rate of about 25 °C/h to room temperature in order to obtain polycrystalline $CuSbTe_2$, $CuSbSe_2$ and $CuSbS_2$ compounds. The thin films of these compounds were prepared by thermal evaporation from a molybdenum boat under vacuum of 1.3 mPa (10^{-5} Torr) onto glass substrates at 300 K at a rate of about 30 nm/min, using the coating unit Leybold-Heraeus Univex-300.

The thickness of the films was measured using an optical multiple-beam interferometer.

The crystal structures of $CuSbTe_2$, $CuSbSe_2$ and $CuSbS_2$ in both powder and thin-film forms were investigated by the X-ray diffractometer Philips PW 1373.

The composition of the powder samples and of the corresponding thin films of $CuSbTe_2$, $CuSbSe_2$ and $CuSbS_2$ were determined by electron microprobe analysis with an accuracy of about 2%.

The electrical conductivity σ was measured by the conventional four-probe method. The Hall voltage was measured potentiometrically with the usual precautions of reversing both the magnetic and current directions. The thermo-electrical power was measured simultaneously against copper while establishing a maximum temperature gradient of 10 K along the sample. The measured properties were monitored until they were found to be time independent.

3. *Result and discussion*

3.1. *Structural*

The X-ray diffraction patterns of the powder and of the thin films of $CuSbTe_2$, $CuSbSe_2$ and $CuSbS_2$, as deposited and annealed at 373 K and 473 K under vacuum for one hour, are shown in Figs. 1, 2 and 3, respectively. From the X-ray powder diffraction patterns of these compounds, as shown in Fig. 1a, one can calculate the lattice parameters and the corresponding (hkl) planes using the Treior program. Also, the interplane spacing (d), and the positions and heights of the peaks were calculated. The results show that the prepared $CuSbTe_2$, $CuSbSe_2$ and $CuSbS_2$ in a bulk form have the orthorhombic crystal structure. These results agree well with what was reported by other authors [10,12]. The interplane spacing (d) with the corresponding (hkl) planes, and the positions and heights of the peaks are listed in Table 1. The lattice-parameter values and the unit-cell volumes of the three compounds are summarized in Table 2.

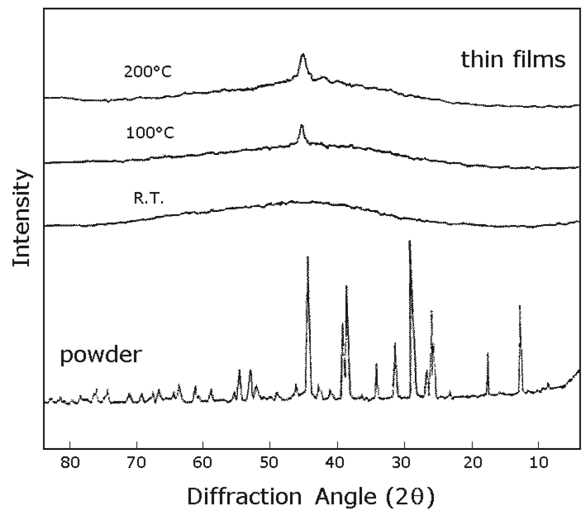

Fig. 1. X-ray diffraction patterns of $CuSbTe_2$.

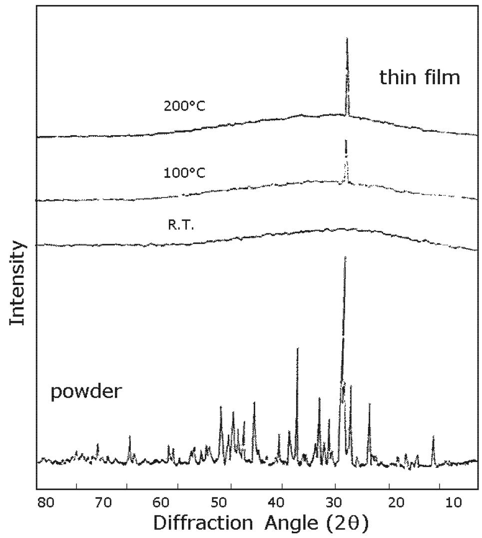

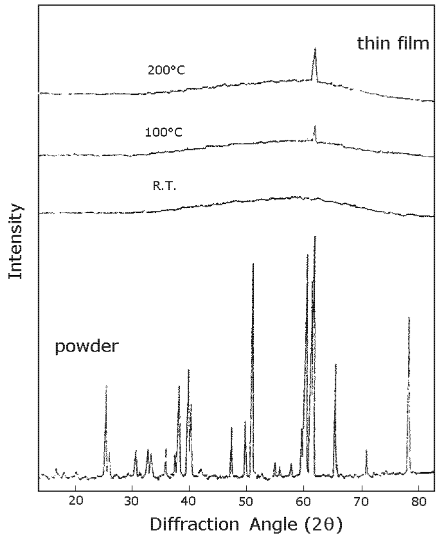

Fig. 2. X-ray diffraction patterns for $CuSbSe_2$.

Fig. 3 (right). X-ray diffraction patterns for $CuSbS_2$.

TABLE 1. Values of d-spacings, diffracion angles, relative intensities and plane indices of $CuSbTe_2$, $CuSbSe_2$ *and* $CuSbS_2$ *in powder forms.*

$CuSbTe_2$			
d (nm)	2θ	I/I'	hkl
0.69104	12.802°	58.95	210
0.50351	17.567°	34.71	400
0.35038	25.391°	42.57	201
0.34769	25.596°	64.4	011
0.30765	29.034°	100	520
0.28644	31.215°	47.58	411
0.26347	34.004°	29.47	511
0.20563	43.991°	98.25	721
0.17394	52.804°	28.37	122
0.16852	54.397°	26.19	151

$CuSbSe_2$			
d (nm)	2θ	I/I'	hkl
0.37668	23.589°	38.39	101
0.32997	27.011°	46.71	020
0.31401	28.409°	100	510
0.31186	28.6°	60.99	211
0.28824	30.98°	31.51	320
0.27122	33.009°	41.38	610
0.23541	38.184°	30.49	601
0.19184	47.397°	30.61	621
0.18504	49.204°	35.37	012
0.17635	51.803°	36.16	901

$CuSbS_2$			
d (nm)	2θ	I/I'	hkl
0.71324	12.4°	66.89	101
0.31401	28.4°	100	020
0.35974	28.8°	81.03	510
0.30155	29.6°	86.2	211
0.22907	39.38°	87.58	320
0.18215	49.8°	33.56	610
0.18159	50.2°	48.27	601
0.17572	52°	55.17	621
0.14416	64.6°	40.34	012

TABLE 2. Values of lattice parameters and unit-cell volumes of $CuSbTe_2$, $CuSbSe_2$ *and* $CuSbS_2$ *thin films.*

Sample	Lattice parameters			Unit cell volume
	a	b	c	(nm^3)
$CuSbTe_2$	20.17786	9.481876	3.737931	0.71516
$CuSbSe_2$	17.84687	6.595556	3.855409	0.45382
$CuSbS_2$	16.95968	7.130192	6.649178	0.80406

It was found that the calculated lattice parameter values are in good agreement with the standard (JCPPS) diffraction data 1996 card for $CuSbS_2$. The results also agree well with those reported by Deshpande et al. [11] and by Bastow and Whitfield [9].

From Figs. 1, 2 and 3, it was observed that the as-deposited films were amorphous, whilst those heat-treated at 373 K and 473 K were polycrystalline. It was also observed that the peak intensity and the peak width at half amplitude appreciably at higher annealing temperatures which gives information about the degree of preferred orientation and the degree of crystallinity concerning the crystalline planes (211) in $CuSbTe_2$, (301) in $CuSbSe_2$ and (520) in $CuSbS_2$, as represented in Figs. 1, 2 and 3, respectively.

The compositions of the powder samples and of the corresponding thin films of the three compounds were determined by electron microprobe analysis with an accuracy of ±2%. The results of the compositional analysis are reported in Table 3. These results confirm the results obtained by the X-ray analysis.

TABLE 3. Composition of $CuSbTe_2$, $CuSbSe_2$ *and* $CuSbS_2$ *powder and thin films.*

Sample	Powder					Thin film				
	Cu	Sb	Te	Se	S	Cu	Sb	Te	Se	S
$CuSbTe_2$	25.20	25.59	49.22			24.89	24.99	50.12		
$CuSbSe_2$	24.94	25.42		49.64		24.88	25.23		49.89	
$CuSbS_2$	25.12	25.03			49.84	24.79	25.00			50.21

The $CuSbTe_2$, $CuSbSe_2$ and $CuSbS_2$ thin films were also investigated by the transmission electron microscopic technique in order to get more information about their structure.

Figures 4a, b and c represent selected areas of the transmission patterns for the $CuSbTe_2$, $CuSbSe_2$ and $CuSbS_2$ thin films, as-deposited and annealed at 373 K and 473 K in vacuum for one hour. From these patterns, it is clear that the grain size of the material increases when increasing the annealing temperature. This means that the thin films of these compounds changed from the amorphous to the crystalline state by heat treatment.

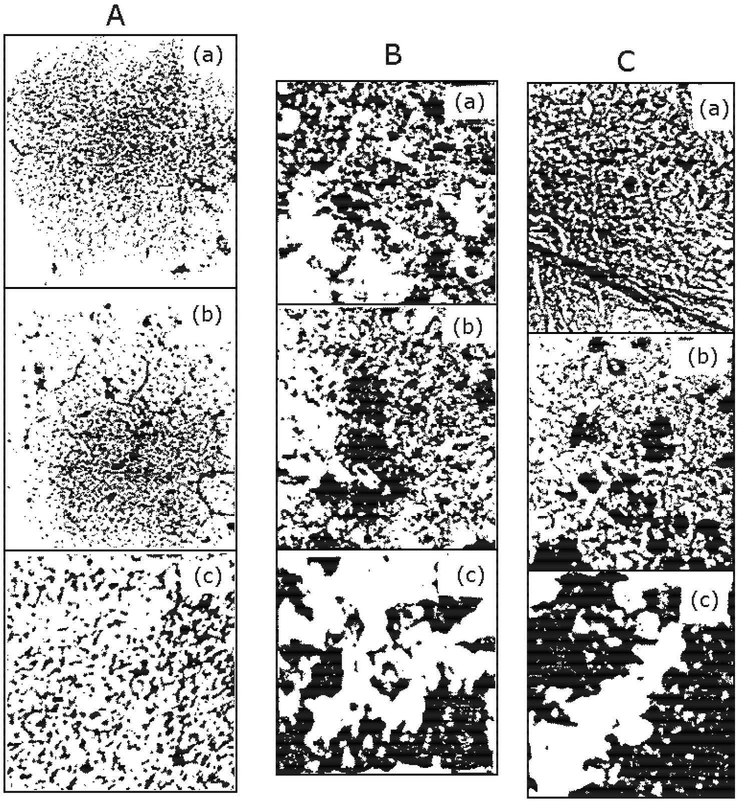

Fig. 4. Electron-microscope transmission patterns of A: $CuSbTe_2$, *B:* $CuSbSe_2$ *and C:* $CuSbS_2$ *thin films, (a): as-deposited, (b): annealed at 373* K *and (c): annealed at 473* K.

3.2. Electrical properties

It was found that for film thicknesses greater than 150 nm, the variation of electrical conductivity, σ, is negligible and does not exceed $\pm 4\%$. So, we did our electrical measurements with films 154 nm thick.

3.2.1. **Electrical conductivity of $CuSbTe_2$ thin film**

The electrical conductivity, σ, of the prepared $CuSbTe_2$ thin films of thickness 154 nm was measured over the temperature range from 100 K to 500 K.

Figures 5a, b and c show the temperature dependence of the electrical conductivity of the as-deposited $CuSbTe_2$ thin films and those annealed at 373 K and 473 K. From Fig. 5a, it is clear that the conductivity at low temperature is low, because most of the carriers are frozen out on the acceptor and donor levels. As the tempetature rises, the degree of ionization of the impurities increases, and the raise of the carrier concentration results in a rapidly increasing conductivity.

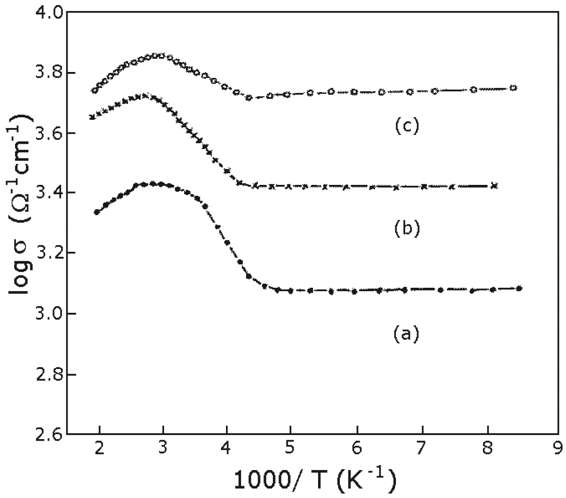

Fig. 5. Inverse temperature dependence of DC conductivity σ of $CuSbTe_2$ *thin films, (a): as-deposited, (b): annealed at 373* K *and (c): annealed at 473* K.

At higher temperature, the conductivity shows a flat maximum at about 348 K, followed at still higher temperature by a tendency to decrease. The reason for the tendency lies in the temperature dependence of the mobility; in this temperature range, the films exhibit a metallic behaviour. In this temperature range, the mobility of the carriers decreases with a raising temperature because of the lattice

TABLE 4. Values of the activation energies ΔE_1 and ΔE_2 of the as-deposited, and annealed at 373 K *and 473* K *thin films of* $CuSbTe_2$, $CuSbSe_2$ *and* $CuSbS_2$.

Sample	Activation energy eV	
	ΔE_1	ΔE_2
$CuSbTe_2$ as-deposited	0.0672	
$CuSbTe_2$ annealed at 373 K	0.0461	
$CuSbTe_2$ annealed at 473 K	0.022	
$CuSbSe_2$ as-deposited	0.17	0.0329
$CuSbSe_2$ annealed at 373 K	0.09	0.0219
$CuSbSe_2$ annealed at 473 K	0.052	0.0204
$CuSbS_2$ as-deposited	0.285	0.093
$CuSbS_2$ annealed at 373 K	0.229	0.067
$CuSbS_2$ annealed at 473 K	0.177	0.061

scattering. The increasing thermal agitation of the lattice causes shorter distances of the carriers between collisions, and the carriers travel faster, thus reducing the time between collisions. Both these facts cause the decrease of the mobility.

Figures 5a, b and c show that all films, as-deposited and annealed at different temperatures, have the same behaviour, but the annealing temperature increases only the value of conductivity. This increase of the conductivity is due to the transformation of the as-deposited $CuSbTe_2$ thin films from the amorphous to the crystalline state. The activation energy, as calculated from the curves in Figs. 5a, b and c, are summarized in Table 4. From this table, it is clear that the activation energy decreases when increasing the annealing temperature. This decrease of activation energy with annealing temperature may be attributed to the Cu deficiency.

3.2.2. Electrical conductivity of $CuSbSe_2$ and $CuSbS_2$ thin films

The temperature dependence of the electrical conductivity, σ, of the as-deposited $CuSbSe_2$ and $CuSbS_2$ thin films and those annealed at 373 K and 473 K, is shown in Figs. 6a, b and c and 7a, b and c, respectively.

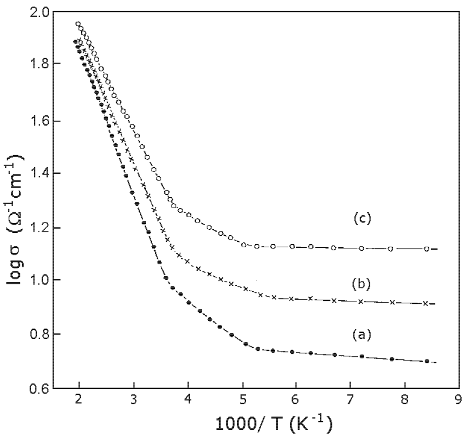

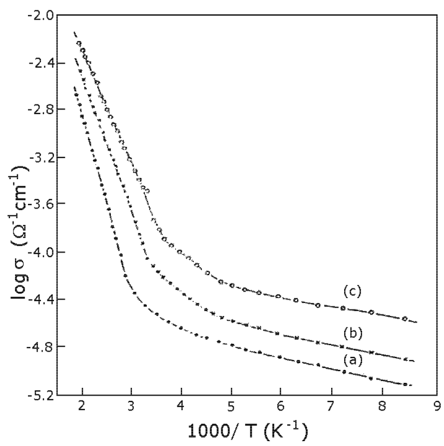

Fig. 6. Inverse temperature dependence of DC conductivity σ of $CuSbSe_2$ *thin films, (a): as-deposited, (b): annealed at 373* K *and (c): annealed at 473* K.

Fig. 7 (right). Inverse temperature dependence of DC conductivity σ of $CuSbS_2$ *thin films, (a): as-deposited, (b): annealed at 373* K *and (c): annealed at 473* K.

The general features of these curves are that the conductivity increases as the temperature increases in the investigated temperature range, which shows a semiconductor behaviour. The results for the temperature range below 178 K can be considered separately from those above 178 K. In the temperature range above 200 K, the conductivity increases exponentially and shows two linear regions, one from (178 K – 288 K) and the other from (288 K – 500 K). It can be represented by the relation

$$\sigma = \sigma_0 \exp(-\Delta E/kT),$$

where σ_0 is the pre-exponential factor, ΔE is the conductivity activation energy, k is the Boltzmann's constant and T is the absolute temperature.

From Figs. 6 and 7, it is also clear that the increasing rate of the conductivity is greater at high temperature than at low temperature. The values of the activation energy, ΔE, calculated from the corresponding slopes (ΔE_1 and ΔE_2) for the as-deposited $CuSbSe_2$ and $CuSbS_2$ thin films and those annealed at 373 K and 473 K, are summarized in Table 4. It is clear from these results that both activation energies, ΔE_1 and ΔE_2, decrease with increasing the annealing temperatures for $CuSbSe_2$ and $CuSbS_2$ thin films. Such behaviour may be attributed to the Cu deficiency, which leads to the implantation of acceptor levels within the forbidden gap. These acceptor levels occupy two different localized states within the energy gap: one is very close to the conduction band, while the other is deeper. Such two different localized-state activation energies, one at low temperatures (178 K – 288 K), ΔE_1, corresponds to the shallow levels while the other, ΔE_2 at high temperatures (288 K – 500 K), corresponds to the deeper levels. As the annealing temperature increases, broadening of both acceptor levels may happen which consequently decreases the activation energy. In the low-temperature region below 178 K, the slope of the curves, as shown in Figs. 6 and 7, continuously decreases with increasing temperature. This means that the dependence of $\log\sigma$ on $1/T$ is nonlinear. In this case, the conduction takes place through the Mott's variable-range hopping (VRH) mechanism. This can be verified by the following relation [16]

$$\sigma = \frac{\sigma_0}{T^{1/2}} \exp(-(T_0/T)^{1/4}),$$

where T_0 is the degree of disorder.

Figures 8a, b and c and 9a, b and c represent the plot of $\log\sigma T^{1/2}$ versus $(1/T)^{1/4}$ for the as-deposited $CuSbSe_2$ and $CuSbS_2$ and those annealed at 373 K and 473 K. From these curves it is clear that $\log\sigma T^{1/2}$ versus $(1/T)^{1/4}$ is a linear relation. This is in good accordance with the Mott's (VRH) process. The localized states necessary for such a conduction process are a consequence of imperfections associated with the polycrystalline films [17]. It is also well known that in this case T_0 is related to the density of a localized state near the Fermi level $g(f)$ by the equation

$$g(f) = 16\alpha_0^3/kT_0,$$

where α_0 is the special extension of the wave function associated with the localized state, T_0 is the degree of disorder and

$$\sigma\alpha_0 = 3\,e^2\,\nu_{\rm ph}\big[g(f)/8\pi\alpha_0\,k\big],$$

where $\nu_{\rm ph} = 10^{13}$ Hz is the characteristic phonon frequency in most amorphous materials. The average hopping distance R and the hopping energy W are given

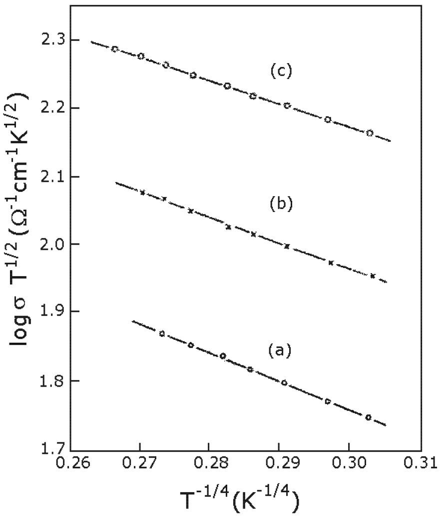

Fig. 8. Plot of $\log\sigma T^{1/2}$ *vs.* $T^{-1/4}$ *for* $CuSbSe_2$ *thin films, (a): as-deposited, (b): annealed at 373* K *and (c): annealed at 473* K.

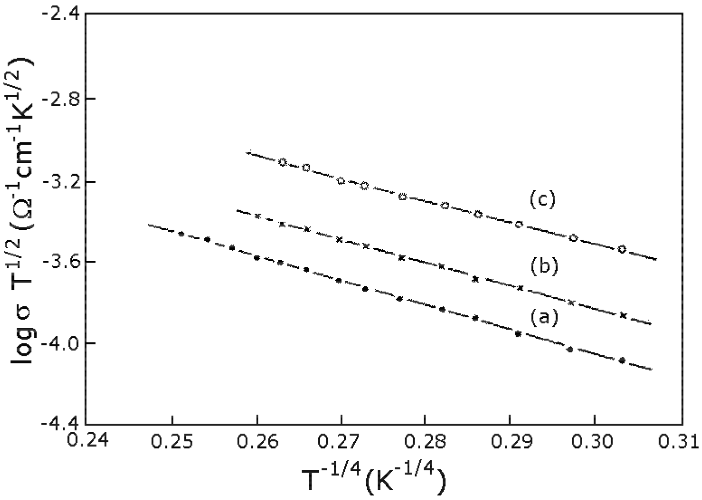

Fig. 9 (right). Plot of $\log\sigma T^{1/2}$ *vs.* $T^{-1/4}$ *for* $CuSbS_2$ *thin films, (a): as-deposited, (b): annealed at 373* K *and (c): annealed at 473* K.

by the expressions [18]

$$R = \left[\frac{9}{8\pi\alpha_0 kTg(f)}\right]^{1/4} ,$$

$$W = \frac{3}{4\pi R^3 g(f)} .$$

The calculated values of σ_0, T_0, α_0, $g(f)$ and W are given in Table 5. From Table 5, it was found that $g(f)$ increases when increasing the annealing temperature for $CuSbTe_2$, $CuSbSe_2$ and $CuSbS_2$ thin films.

TABLE 5. Values of the constant σ_0, degree of disorder T_0, constant α_0, function $g(f)$, average hopping distance R and hopping energy W of as-deposited, and annealed at 373 K *and 473* K *thin films of* $CuSbSe_2$ *and* $CuSbS_2$.

Sample (see B)	σ_0 (see A)	T_0 (K)	α_0 (cm^{-1})	$g(f)$ ($eV^{-1}cm^{-3}$)	R (cm)	W (10^{-4} eV)
1	724.435	190.268	2250.810 $\times 10^9$	1115.063 $\times 10^{37}$	0.02017 $\times 10^{-10}$	0.02608
2	1202.264	167.961	3509.601 $\times 10^9$	4788.739 $\times 10^{37}$	0.01254 $\times 10^{-10}$	0.02527
3	1548.816	104.857	3572.402 $\times 10^9$	8089.387 $\times 10^{37}$	0.01095 $\times 10^{-10}$	0.02246
4	26.910 10^{-2}	22577	910.950 $\times 10^7$	622.920 $\times 10^{28}$	0.02926 $\times 10^{-7}$	1.529
5	39.810 10^{-2}	17581	1189.011 $\times 10^7$	1778.810 $\times 10^{28}$	0.02106 $\times 10^{-7}$	1.436
6	50.111 10^{-2}	15735	1416.110 $\times 10^7$	3357.700 $\times 10^{28}$	0.01720 $\times 10^{-7}$	1.396

A. ($\Omega^{-1}cm^{-1}K^{-1}$)

B.
1. $CuSbSe_2$ as-deposited
2. $CuSbSe_2$ annealed at 373 K
3. $CuSbSe_2$ annealed at 473 K
4. $CuSbS_2$ as-deposited
5. $CuSbS_2$ annealed at 373 K
6. $CuSbS_2$ annealed at 373 K

3.2.3. **Hall effect**

The Hall effect has been investigated for the annealed $CuSbTe_2$, $CuSbSe_2$ and $CuSbS_2$ thin films in the temperature range from 300 to 500 K. The values of the Hall coefficient R_H for all investigated films are positive indicating p-type conduction. Therefore, the majority of the charge carriers in these films are free holes. This may be due to Cu vacancies. The carrier concentration P for $CuSbTe_2$, $CuSbSe_2$ and $CuSbS_2$ thin films can be calculated using the relation

$$P = \frac{1}{eR_H} ,$$

where R_H is the Hall coefficient.

The calculated values of P for $CuSbS_2$ changed from 2.26×10^{16} cm^{-3} to 1.37×10^{17} cm^{-3} indicating non-degeneracy over the measured temperature range, while in $CuSbSe_2$, P changed from 5.77×10^{18} cm^{-3} to 1.6×10^{19} cm^{-3}, indicating that $CuSbSe_2$ thin films are partially degenerate in the temperature range from 300 K to 500 K. In the case of $CuSbTe_2$, P slightly changed from 1.98×10^{19} cm^{-3} to 2.22×10^{19} cm^{-3}, indicating degeneracy in the temperature range from 360 K to 500 K in which the Hall coefficient is nearly constant.

3.2.4. **Thermoelectric power**

Figure 10 represents the relation between the thermoelectric power Q and temperature for the annealed $CuSbTe_2$, $CuSbSe_2$ and $CuSbS_2$ thin films. From these curves, it is found that the three films under investigation were p-type over the measured temperature range, which is in agreement with the Hall effect. It is also clear that Q increases with increasing temperature for $CuSbTe_2$, $CuSbSe_2$ and $CuSbS_2$ thin films, indicating a typical semiconducting behaviour. Its values vary from 0.02 mV/°C to 0.19 mV/°C on going from 300 K to 500 K for $CuSbTe_2$, from 0.03 mV/°C to 0.26 mV/°C for $CuSbSe_2$ and from 0.05 mV/°C to 0.34 mV/°C for $CuSbS_2$ in the same temperature range. These results are in good agreement with the results obtained by Aliev et al. [18].

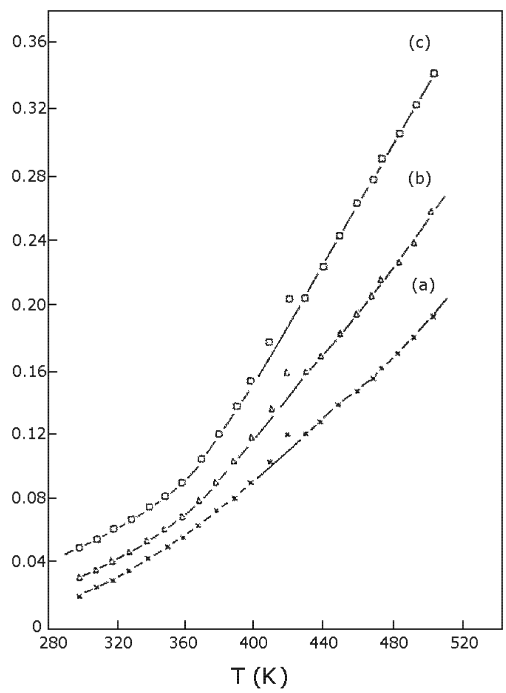

Fig. 10. Temperature dependence of the thermoelectric power Q of the annealed films of (a): $CuSbTe_2$, *(b):* $CuSbSe_2$ *and (c):* $CuSbS_2$.

The temperature dependence of m^*/m_0 for the annealed $CuSbTe_2$, $CuSbSe_2$ and $CuSbS_2$ thin films in the temperature range 300 to 500 K is shown in Fig. 11. It can be seen that m^* increases as the temperature T increases.

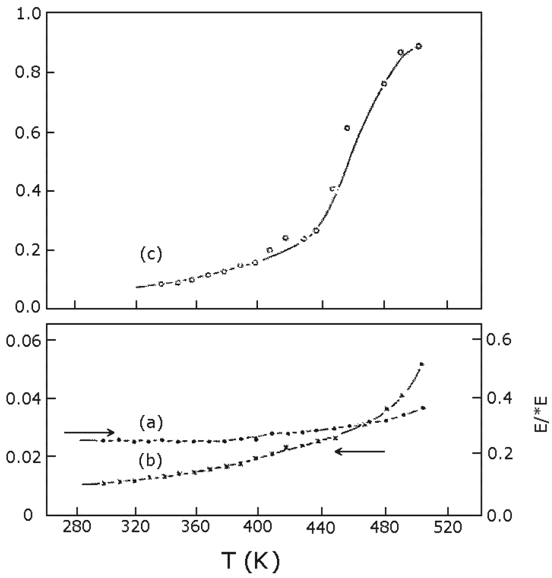

Fig. 11. Temperature dependence of the effective mass m^*/m_0 in (a): $CuSbTe_2$, *(b):* $CuSbSe_2$ *and (c):* $CuSbS_2$.

4. Conclusion

The structural and electrical properties of the ternary chalcogenides $CuSbTe_2$, $CuSbSe_2$ and $CuSbS_2$, prepared by the fusion method, have been studied. Thin films of these compounds were obtained by thermal evaporation on glass substrates. It has been demonstrated that the obtained films are of amorphous structure at room temperature and become polycrystalline by heat treatment under vacuum of 1.3 mPa (10^{-5} Torr) for one hour at 373 K and 473 K. X-ray diffraction measurements show that $CuSbTe_2$, $CuSbSe_2$ and $CuSbS_2$ compounds have orthorhombic structure. It was found that the conductivity, σ, increases while the activation energy decreases with temperature. Thermoelectric power and Hall voltage measurements indicate that the majority of carriers are holes for all thin films (p-type conduction). The temperature dependence of the thermoelectric power, and consequently of electrical conduction, showed that the films were markedly non-degenerate semiconductors for $CuSbS_2$ thin films and partially degenerate for $CuSbSe_2$ thin films, while $CuSbTe_2$ thin films were degenerate semiconductors.

References

[1] M. J. Thwaites, R. D. Tolinson and M. J. Hamphire, Solid State Commun. **23** (1977) 905.

[2] E. Conwell and V. Weiskopf, Phys. Rev. **11** (1950) 388.

[3] V. P. Zhuze, V. M. Sergeeva and E. L. Shteum, Soviet Phys. Techn. Phys. **3** (1958) 1925.

[4] J. L. Shay and J. H. Wernick, *Ternary Chalcopyrite Semiconductors*, Pergamon Press, New York (1975).

[5] W. Hofmann, Z. Kristallogr. **68** (1932) 84177.

[6] K. A. Sharaf, N. Abdel Mohsen, S. Naser and A. H. Abou El Ela, Acta Physica Hungarica **70** (1991) 56.

[7] L. I. Berger and V. D. Prochukan, *Ternary Diamond-Like Semiconductors*, Consultant Bureau Enterprises. Inc., New York (1969) 47.

[8] V. P. Zhuze, V. M. Sergeeva and E. L. Shtrum, Soviet Phys. Techn. Phys. **3** (1925) 1925.

[9] T. J. Bastow and H. J. Whitfield, J. Solid State Chem. **40** (1981) 203.

[10] Y. Nakamura and M. Shimoji, Trans. Faraday Soc. (1969) 1509; Y. Nimomiya, Y. Nakamura, T. Itami and M. Shimoji, Trans. JIM **13** (1972) 259.

[11] A. P. Deshpande, V. B. Sapre and C. Mand, J. Phys. C: Solid State Phys. **17** (1984) 955.

[12] Y. Ninoniya, Y. Nakamura and M. Shimoji, J. Non-Cryst. Solids, **17** (1975) 231.

[13] K. A. Sharaf, N. Abdel Mahsen, S. Naser and A. H. Abou El Ela, Fizika A (Zagreb) **23** (1991) 317.

[14] A. R. Regel, A. A. Andreev, B. A. Kotov, M. Mamdaliev, N. M. Okuneva, I. A. Smirnov and E. V. Shadrich, J. of Non-Cryst. Solids **4** (1970) 151.

[15] S. S. Dhumure and C. D. Lokhande, Indian J. Pure Appl. Phys. 31 (1993) 512.

[16] E. David, Z. f. Phys. 106 (1937) 106.

[17] R. M. Mera, R. Kumar and P. C. Mathur, Thin Solid Films **170** (1989) 15.

[18] S. N. Aliev, G. G. Gadzhiev and Ya. B. Magomedov, Soviet Phys. Semiconductors **3** 11 (1970) 1437.

STRUKTURNA I ELEKTRIČNA SVOJSTVA TANKIH SLOJEVA KALKOGENIDA $CuSbTe_2$, $CuSbSe_2$ AND $CuSbS_2$

Trokomponentne smo kalkogenide $CuSbTe_2$, $CuSbSe_2$ and $CuSbS_2$ pripremili metodom talenja. Tanke smo slojeve tih spojeva pripremali isparavanjem u vakuumu od oko 1.3 mPa, brzinom nanošenja oko 30 nm/min. Strukturna svojstva tih kalkogenida, kako praškova, tako i tankih slojeva, istraživali smo difrakcijom rendgenskog zračenja i prolaznom elektronskom mikroskopijom. Pomoću mikroprobe odredili smo kemijski sastav spojeva i njihovih tankih slojeva. Izmjerili smo električnu vodljivost, σ, i termoelektričnu snagu, Q, svih svježe naparenih i opuštenih legura i njihovih tankih slojeva u ovisnosti o temperaturi u području 80 do 500 K. Električna vodljivost, gustoća nositelja, P, mobilnost, μ, i termoelektrična snaga , Q,povećavaju se ako se tanki slojevi opuštaju na višim temperaturama. Povećanje σ, P, μ and Q, a također smanjenje aktivacijske energije, ΔE, u tankim slojevima $CuSbTe_2$, $CuSbSe_2$ i $CuSbS_2$ tumače se promjenama strukture tih slojeva od amorfnog u kristalinično stanje.